JACS
JOURNAL OF THE AMERICAN CHEMICAL SOCIETY
Article
Cite This: J. Am. Chem. Soc. 2019, 141, 11970−11975
pubs.acs.org/JACS

A Dimeric Hydride-Bridged Complex with Geometrically Distinct Iron Centers Giving Rise to an $S = 3$ Ground State

Anne K. Hickey,[†] Samuel M. Greer,[‖,§] Juan A. Valdez-Moreira,[†] Sean A. Lutz,[†] Maren Pink,[†] Jordan A. DeGayner,[‡] T. David Harris,[‡] Stephen Hill,[‖,^] Joshua Telser,[∥] and Jeremy M. Smith*[,†]

[†]Department of Chemistry, Indiana University, 800 East Kirkwood Avenue, Bloomington, Indiana 47405, United States
[‖]National High Magnetic Field Laboratory, Florida State University, Tallahassee, Florida 32310, United States
[§]Department of Chemistry & Biochemistry and [^]Department of Physics, Florida State University, Tallahassee, Florida 32306, United States
[‡]Department of Chemistry, Northwestern University, Evanston, Illinois 60208, United States
[∥]Department of Biological, Physical and Health Sciences, Roosevelt University, Chicago, Illinois 60605, United States

Supporting Information

ABSTRACT: Structural and spectroscopic characterization of the dimeric iron hydride complex $[Ph_2B(^tBuIm)_2FeH]_2$ reveals an unusual structure in which a tetrahedral iron(II) site ($S = 2$) is connected to a square planar iron(II) site ($S = 1$) by two bridging hydride ligands. Magnetic susceptibility reveals strong ferromagnetic coupling between iron centers, with a coupling constant of $J = +110(12)$ cm^{-1}, to give an $S = 3$ ground state. High-frequency and -field electron paramagnetic resonance (HFEPR) spectroscopy confirms this model. A qualitative molecular orbital analysis of the electronic structure, as supported by electronic structure calculations, reveals that the observed spin configuration results from the orthogonal alignment of two geometrically distinct four-coordinate iron fragments held together by highly covalent hydride ligands.

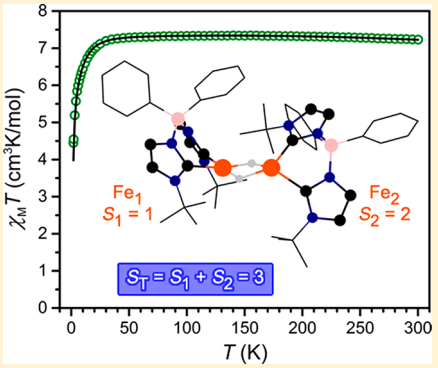

INTRODUCTION

Over the past several decades, substantial efforts have been directed toward the study of multinuclear magnetic molecules in which diamagnetic bridging ligands mediate superexchange coupling between paramagnetic metal ions.[1] The nature and magnitude of this coupling is quantified by the exchange constant, J, which is correlated to the energetic separation of the ground state and excited states. Within the field of molecular magnetism, the development of general strategies to maximize the magnitude of J represents a central challenge to synthetic chemists, as strong coupling is necessary to maintain collective intramolecular magnetic behavior at high temperature.[2] Because the strength of magnetic exchange between two paramagnetic centers drops precipitously with distance, single-atom bridges provide the ultimate limit in maximizing superexchange interactions. For instance, oxo-bridged complexes often exhibit magnitudes of J that are well in excess of 100 cm^{-1}.[3]

The small size of the hydride ion renders it an ideal bridging ligand for mediating strong superexchange interactions between metal centers. Furthermore, the propensity of hydride to bridge metal ions has long been recognized,[4] although the vast majority of these complexes feature diamagnetic metal centers. It is only recently, with the development of ligands that stabilize low-coordinate metal centers,[5] that paramagnetic metal hydride complexes, in some cases featuring bridging hydrides, have become readily accessible. Nonetheless, only a limited number of studies on the magnetic properties of these complexes have been reported.[6] Most notably, strong antiferromagnetic coupling was observed for a chromium(II) hydride dimer[7] and for a triangular cobalt(I) hydride trimer,[8] while strong intramolecular, noncompensated antiferromagnetic coupling was reported for a remarkable mixed-valence tetranuclear chromium hydride cluster.[9] In addition, the delocalized bonding of the $Ni_2(\mu\text{-}H)_2$ core led to an unusual $S = 1$ ground spin state in $[Cp'NiH]_2$ (Cp′ = 1,2,3,4-tetraisopropylcyclopentadienyl).[10] Finally, antiferromagnetic coupling mediated through bridging hydrides between cobalt(II) centers in the solid-state compound $LaSrCoO_3H_{0.7}$ was shown to engender a bulk ferrimagnet with a Néel temperature of $T_N \geq 350$ K.[11]

We have previously reported the ability of bulky bis(carbene)borate ligands to stabilize coordinatively unsaturated iron complexes, akin to the commonly used β-diketiminate ligands, but with significantly greater donor strength.[12,13] Given that strongly donating ligands are known to stabilize iron(II) in a square planar geometry,[14] we hypothesized that

Received: April 23, 2019
Published: July 8, 2019

DOI: 10.1021/jacs.9b04389
J. Am. Chem. Soc. 2019, 141, 11970−11975

access to this geometry may similarly occur in a hydride-bridged diiron bis(carbene)borate complex, resulting in unusual magnetic properties. This would be in contrast to the β-diketiminate congeners, where each iron ion resides in a distorted tetrahedral-like geometry.[15] In this report, we describe the synthesis and spectroscopic and magnetic properties and provide a description of the electronic structure of a hydride-bridged diiron bis(carbene)borate complex, wherein strong ferromagnetic coupling between the two iron centers is observed. To our knowledge, this complex provides the first example of ferromagnetic coupling through the hydride ligand.

RESULTS AND DISCUSSION

The previously reported iron(II) chloride complex $Ph_2B(^tBuIm)_2FeCl(THF)$[12] reacts with equimolar $NaBEt_3H$ to yield the dark blue, hydride-bridged dimeric complex $[Ph_2B(^tBuIm)_2FeH]_2$ in 88% yield. The molecular structure of the complex, as determined by single-crystal X-ray diffraction, reveals an unusual geometry (Figure 1). As exemplified by β-diketiminate complexes,[15] dinuclear complexes with an $Fe(\mu\text{-}H)_2Fe$ core generally feature low-coordinate iron centers in equivalent coordination geometries, whereas the two iron centers of $[Ph_2B(^tBuIm)_2FeH]_2$ are distinct, despite each having the same inner coordination sphere. Specifically, Fe(1) resides in a tetrahedral-like environment (τ_4 = 0.7), while Fe(2) is in a square-planar environment (τ_4 = 0.1).[16,17] This complex thus constitutes a rare example of a hydride dimer comprising geometrically distinct monomers.[18] While we were unable to observe Fe−H vibrations spectroscopically,[19] high resolution mass spectrometry of $[Ph_2B(^tBuIm)_2FeH]_2$ and its deuterated isotopologue, $[Ph_2B(^tBuIm)_2FeD]_2$, combined with the results of preliminary reactivity studies, support the presence of the hydride ligands.[20]

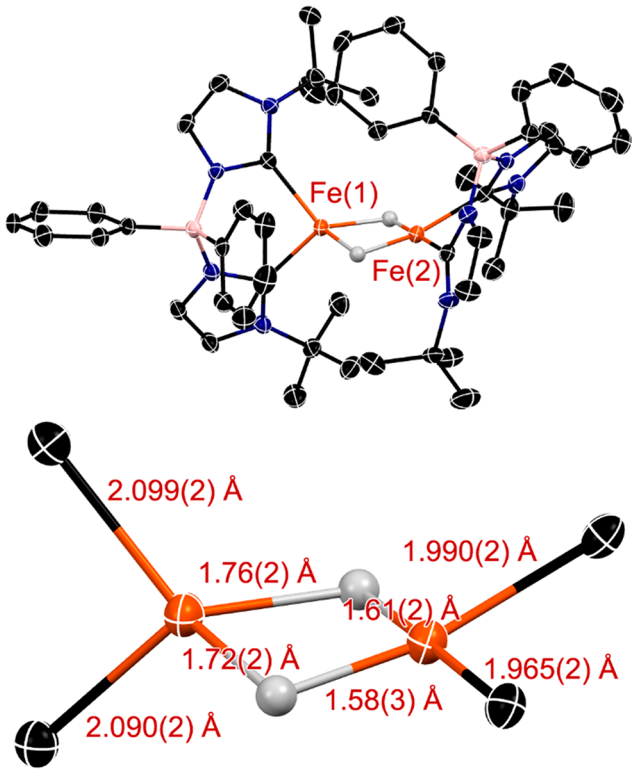

Figure 1. Top: X-ray crystal structure of $[Ph_2B(^tBuIm)_2FeH]_2$. Thermal ellipsoids shown at 50% probability; peripheral hydrogen atoms omitted for clarity. Bottom: Core structure of the molecule, with selected bond lengths. Black, white, blue, pink, and orange ellipsoids represent carbon, hydrogen, nitrogen, boron, and iron atoms, respectively.

The bond metrics reflect the different coordination environments of the iron centers, with the metal−ligand bond lengths involving Fe(1) being longer than those for Fe(2). While the Fe(1)−H bonds are similar to those in related complexes,[15] the Fe(2)−H bonds are shorter. As a consequence of the shorter bond lengths involving Fe(2), the Fe(1)−Fe(2) distance in $[Ph_2B(^tBuIm)_2FeH]_2$ (2.5247(4) Å) is slightly shorter than that observed for related iron(II) β-diketiminate complexes (average Fe−Fe distance = 2.56(7) Å).[15] Furthermore, the Fe−C bond lengths at Fe(1) are similar to those observed for four-coordinate high-spin (S = 2) iron(II) N-heterocyclic carbene complexes, while those for Fe(2) are similar to those observed for S = 1 square planar iron(II) complexes.[14] These metrics suggest that the core of the complex is composed of a tetrahedral iron(II) (S = 2) center that is linked to a square planar iron(II) center (S = 1) by two bridging hydride ligands. However, alternative formulations involving a redox change (i.e., disproportionation), such as square planar Fe(I) and tetrahedral Fe(III), both of which have been previously observed, cannot be excluded solely on the basis of the structural data.

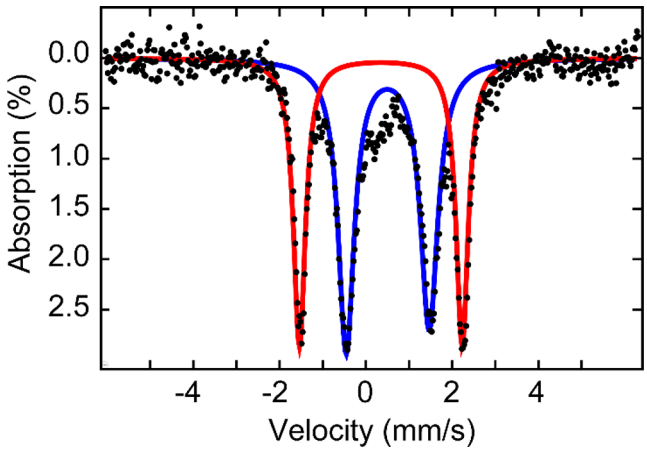

Figure 2. Solid-state Mössbauer spectrum of $[Ph_2B(^tBuIm)_2FeH]_2$ at 80 K. Black circles represent experimental data, while red and blue lines correspond to fits of subspectra I and II, respectively (see text for fit parameters).

Given this ambiguity, we used ^{57}Fe Mössbauer spectroscopy to provide insight into the oxidation states of the two iron centers. As expected for the nonsymmetric structure, the zero-field spectrum of solid $[Ph_2B(^tBuIm)_2FeH]_2$ indicates two different iron environments (Figure 2). The isomer shift (δ = 0.35 mm/s) and large quadrupole splitting (ΔE_Q = 3.77 mm/s) in subspectrum I are both similar to the spectral data of previously reported organometallic S = 1 square planar iron(II) complexes.[14] In contrast, the isomer shift (δ = 0.51 mm/s) and quadrupole splitting (ΔE_Q = 1.92 mm/s) of subspectrum II are similar to established examples of tetrahedral S = 2 iron(II) N-heterocyclic carbene complexes.[14b,c] The spectral parameters for this subspectrum are also very similar to those observed for dinuclear β-diketiminate

DOI: 10.1021/jacs.9b04389
J. Am. Chem. Soc. 2019, 141, 11970−11975

iron(II) hydride complexes.[15d−f] Alternative fits to the data gave nonreasonable parameters, particularly for the quadrupole splitting.[19] The Mössbauer spectral data therefore confirm that the complex contains two iron(II) centers, one of which is tetrahedral (S = 2) and the other square planar (S = 1).[21]

To probe the presence of magnetic interactions between iron(II) centers, variable-temperature dc magnetic susceptibility data were recorded for a solid-state sample of $[Ph_2B(^tBuIm)_2FeH]_2$ under an applied field of 5000 Oe (Figure 3). At 300 K, $\chi_M T$ = 7.23 cm^3 K/mol, which is much

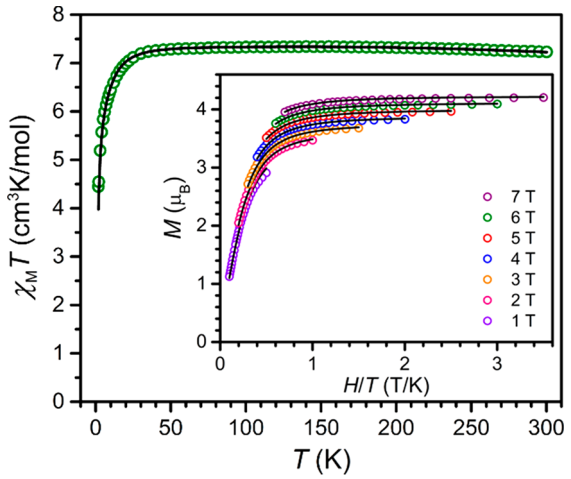

Figure 3. Variable-temperature dc magnetic susceptibility data for $[Ph_2B(^tBuIm)_2FeH]_2$, collected under an applied field of 5000 Oe, with the black line corresponding to a fit of the data. Inset: Low-temperature magnetization data for $[Ph_2B(^tBuIm)_2FeH]_2$, collected at selected fields in the temperature range 2−10 K, with the black lines corresponding to a fit of the data (see text for all fit parameters).

larger than the value of $\chi_M T$ = 4.00 cm^3 K/mol expected for magnetically isolated S = 2 and S = 1 iron(II) centers with g = 2.00. Instead, this value suggests the presence of strong ferromagnetic coupling between iron(II) centers that manifests even up to 300 K. In support of this hypothesis, $\chi_M T$ continues to increase with decreasing temperature, reaching a maximum value of $\chi_M T$ = 7.34 cm^3 K/mol at 155 K. This value falls relatively close to that of $\chi_M T$ = 6.00 cm^3 K/mol expected for an S = 3 ground state, with g = 2.00, arising from ferromagnetic coupling between S = 2 and S = 1 centers. At lower temperatures, $\chi_M T$ undergoes a precipitous decline, likely stemming from a combination of zero-field splitting (zfs),[22] Zeeman splitting, and/or weak intermolecular antiferromagnetic coupling. To quantify the strength of coupling, the data were modeled with the program PHI[23,24] to provide an exchange constant of J = +110(12) cm^{-1}, with g_{iso} = 2.21(1) and D = −7.0(4) cm^{-1}. Note that this axial zfs parameter, D, acts as an average of the two Fe sites; it is an approximation to avoid complicating this model by overparameterization. In actuality, one would expect such distinct coordination environments at each Fe to give quite different single-ion values of D (and likely for g_{iso} as well).

To assess magnetic anisotropy of the S = 3 ground state of $[Ph_2B(^tBuIm)_2FeH]_2$, magnetization data were collected in the temperature range 2−10 K at selected fields from 1 to 7 T. This temperature range should probe only the S = 3 ground state with no convolution from excited states.[25] The splitting of the resulting isofield curves, along with their saturation being well below the expected M = 6.63 μ_B for an S = 3 ground state with g = 2.21, qualitatively demonstrates the presence of significant magnetic anisotropy (Figure 3, inset). To quantify the anisotropy, the data were fit using the program PHI,[23,26] with a fixed g = 2.21, to give an axial zero-field splitting parameter of D = −10.9(1) cm^{-1}. This relatively large magnitude of D for the S = 3 ground state reflects the significant anisotropy associated with iron(II).

High-frequency and -field electron paramagnetic resonance (HFEPR) has been widely applied to metal complexes with S > 1/2, particularly with non-Kramers (integer-spin) ground states.[27] Recognizing that isotopic substitution may change the distance between the two iron centers,[15f,28] and consequently, the extent of magnetic coupling, we applied HFEPR to powder $[Ph_2B(^tBuIm)_2FeH]_2$, as well as to $[Ph_2B(^tBuIm)_2FeD]_2$. In principle a species with S = 3 could exhibit a large number of allowed EPR transitions,[29] but if the zfs is large in magnitude relative to the microwave energy, then this might not be the case. Indeed, both isotopologues show identical spectra, which consist of relatively few transitions at low field at frequencies of 600−630 GHz. The observed HFEPR spectra, including their temperature dependence, can be satisfactorily simulated using an S = 3 spin Hamiltonian with axial and rhombic second order zfs terms, D and E, respectively, and a small, axial fourth-order zfs term,[29] B_4^0. The effect of both E and B_4^0 terms on bulk magnetic properties is minimal but in magnetic resonance (HFEPR) spectra is apparent. The zfs obtained from HFEPR, D = −7.1 cm^{-1}, $|E|$ = 2.1 cm^{-1}, is in reasonable agreement with that from magnetization, particularly in the sign of D. The HFEPR spectra and their analysis are described in detail in Supporting Information.

The large magnitude of J observed for $[Ph_2B(^tBuIm)_2FeH]_2$ is in accord with previous examples of di-,[7,10] tri-,[8] and tetranuclear[9] transition metal complexes supported by bridging hydrides. However, the presence of ferromagnetic coupling is, to our knowledge, unprecedented in hydride-bridged complexes. This coupling scheme likely arises due to orthogonality of spin-bearing d orbitals of the two iron(II) centers, leading to a ferromagnetic alignment of spins via Hund's rules.

The S = 3 spin ground state can be further rationalized via a qualitative molecular orbital diagram (Figure 4).[30] Assuming C_{2v} symmetry for the molecule, the orbital diagram can be constructed starting from two L_2Fe fragments aligned along the Fe−Fe vector (defining the z-axis) and oriented in an orthogonal fashion. For the square planar site, the $3d_{yz}$ orbital is destabilized by interaction with the σ-donor orbitals of the L_2 ligand (Figure 4a), but this destabilization is ameliorated by second-order mixing with the higher energy $4p_y$ orbital. The corresponding interactions for the tetrahedral site involve the $3d_{xz}$ and $4p_x$ orbitals because this site is rotated by 90° relative to the square planar site (Figure 4b). Combining these fragments provides the $L_2Fe\cdots FeL_2$ unit with Fe···Fe orbitals of σ, π, δ symmetry (Figure 4c). Interestingly, while the π-orbitals are isoenergetic, they are polarized in opposite directions due the nature of the $3d$−$4p$ mixing in each of the two iron sites.[31]

While a number of $L_2Fe\cdots FeL_2$ fragment orbitals (Figure 4c) have the appropriate symmetry to interact with the a_1 H 1s combination, the most significant interaction will be with the σ (a_1) orbital (Figure 4d), providing a low-energy bonding orbital ($1a_1$) and a higher-energy orbital with Fe−H antibonding character ($4a_1$). By contrast, only the π (b_2) orbital has the appropriate symmetry to interact with the b_2 H

DOI: 10.1021/jacs.9b04389
J. Am. Chem. Soc. 2019, 141, 11970−11975

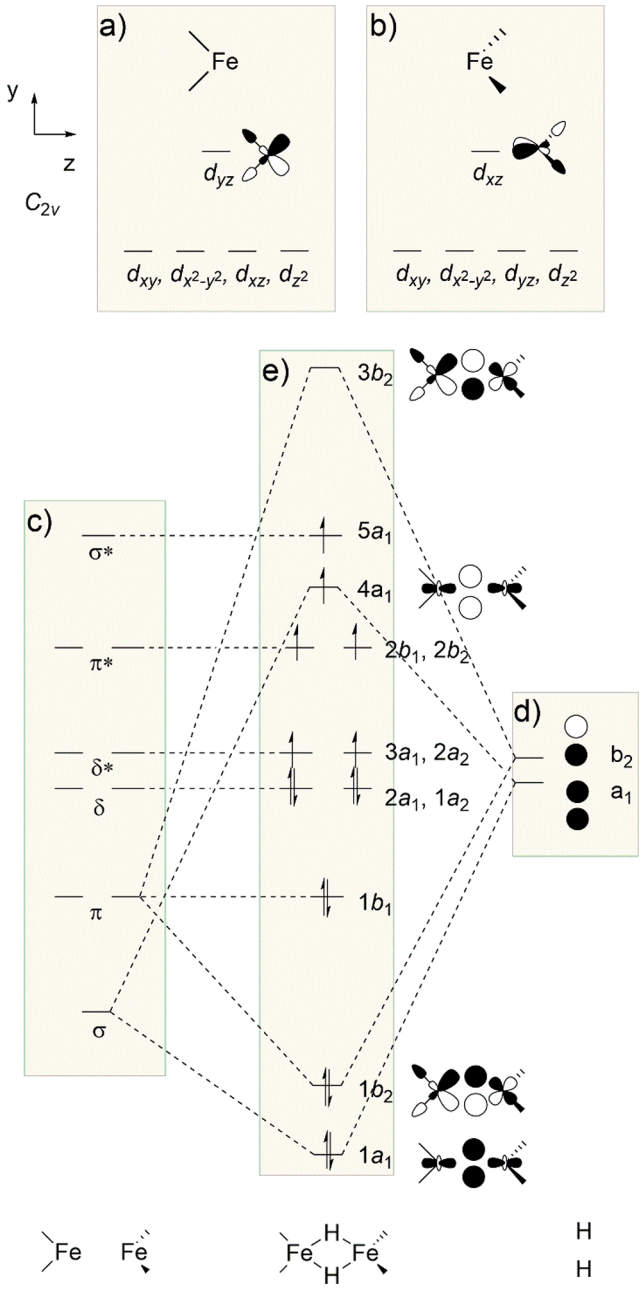

Figure 4. Qualitative MO analysis for $[Ph_2B(^tBuIm)_2FeH]_2$, assuming C_{2v} symmetry and with the $[Fe_2H_2]^{2+}$ core in the *yz* plane. Fragment orbitals for (a) square planar and (b) tetrahedral L_2Fe iron sites, including 3*d*–4*p* mixing, used to construct the fragment orbitals of (c) the $L_2Fe\cdots FeL_2$ fragment. The final MO diagram obtained from mixing this fragment with the 2H fragment orbitals (d) is shown in panel (e). Additional orbital mixing in this low symmetry environment has been ignored in the interest of clarity.

1*s* combination (Figure 4d), providing a low-energy bonding combination ($1b_2$) and a high-energy antibonding combination ($3b_2$). The strong antibonding character of the latter orbital raises it in energy above all of the other $L_2Fe\cdots FeL_2$ fragment orbitals (Figure 4e). Indeed, due to the strong donor abilities of both the bis(carbene)borate and hydride ligands, this orbital is expected to be significantly destabilized, leading to a $5a_1$ and $3b_2$ orbital energy gap that is larger than the spin pairing energy. Accordingly, population of the orbitals with the 16 electrons available to the $[Fe_2H_2]^{2+}$ core is consistent with the experimentally observed $S = 3$ ground state (Figure 4e).

The results of DFT calculations (B3LYP//def2-TZVP Fe, coordinated C,H/def2-svp non-coordinated C,H,N,B) using the crystallographically determined geometry are generally consistent with this qualitative orbital picture. Most notably, the computed LUMO (Figure 5) shows antibonding interactions between the iron atoms and hydrides, similar to those depicted in the $3b_2$ orbital (Figure 4e). While lower-energy orbitals of Fe–Fe σ, π, and δ character can be identified, the relatively low actual symmetry of the molecule leads to extensive orbital mixing that complicates the simple qualitative picture (Figure 4e). The calculated HOMO-LUMO gap is 4.8 eV, and the broken symmetry solution provides a coupling constant of $J = 109$ cm^{-1} (strong coupling formalism),[32] in agreement with the experimentally determined value. Additionally, the computed Mössbauer parameters (B3LYP//CP(PPP) Fe/def2-TZVP coordinated C,H/def2-svp non-coordinated C,H,N,B) for the square planar (δ = 0.15 mm/s and ΔE_Q = 3.89 mm/s) and tetrahedral (δ = 0.37, ΔE_Q = −1.84 mm/s) sites show the same relative magnitudes as those observed experimentally.

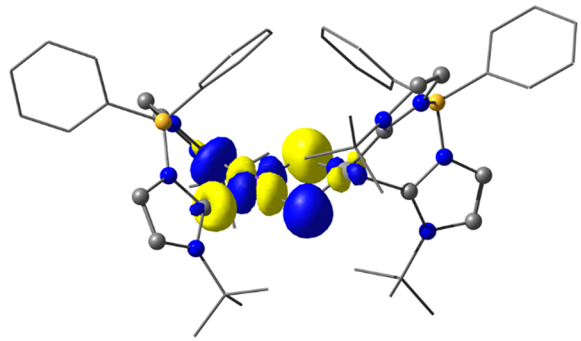

Figure 5. Unrestricted natural orbital representation of the DFT-computed LUMO of $[Ph_2B(^tBuIm)_2FeH]_2$ with orbital isodensity at 0.05.

CONCLUSIONS

The foregoing results demonstrate that the combination of strong donor ability and appropriate steric bulk provided by a bis(carbene)borate ligand stabilizes a unique dinuclear iron(II) hydride-bridged complex exemplifying the two classical four-coordinate geometries: tetrahedral ($S = 2$) and square planar ($S = 1$). Strong ferromagnetic coupling arises from the orthogonal *d*-orbital manifolds of the two iron sites, as mediated by the μ-dihydride bridge. This ferromagnetic exchange can be further rationalized by a qualitative molecular orbital diagram. More generally, these results demonstrate the potential utility of using metal hydride complexes as building blocks for the assembly of high spin clusters. Specifically, through the appropriate choice of metal complexes, we anticipate that the strong bridging ability of the hydride ligand will facilitate the assembly of multinuclear complexes that feature strong ferromagnetic coupling between the constituent metal ions.

ASSOCIATED CONTENT

Supporting Information

The Supporting Information is available free of charge on the ACS Publications website at DOI: 10.1021/jacs.9b04389.

DOI: 10.1021/jacs.9b04389
J. Am. Chem. Soc. 2019, 141, 11970–11975

Full experimental, characterization, and computational details (PDF)

Jmol view of $[Ph_2B(^tBuIm)_2FeH]_2$ (CIF)

AUTHOR INFORMATION

Corresponding Author

*E-mail: smith962@indiana.edu.

ORCID

Samuel M. Greer: 0000-0001-8225-3252

T. David Harris: 0000-0003-4144-900X

Stephen Hill: 0000-0001-6742-3620

Joshua Telser: 0000-0003-3307-2556

Jeremy M. Smith: 0000-0002-3206-4725

Notes

The authors declare no competing financial interest.

ACKNOWLEDGMENTS

The Smith laboratory gratefully acknowledges funding from Indiana University, the National Science Foundation (CHE-1112299, CHE-1566258), and the Department of Energy (DE-SC0019466). Work in the Harris laboratory was funded by the NSF (DMR-1351959) and in the Hill group by the NSF (DMR-1610226). A portion of this work was performed at the National High Magnetic Field Laboratory, which is supported by NSF Cooperative Agreement DMR-1644779 and the State of Florida. We thank Prof. Jesper Bendix, Copenhagen University, for making us aware of the work by Linn and Gibbins, for helpful discussions, and for the program Ligfield. We thank Dr. Andrew Ozarowski, NHMFL, for the EPR simulation program SPIN.

REFERENCES

(1) Gatteschi, D.; Sessoli, R.; Villian, J. *Molecular Nanomagnets*; University Press: Oxford, 2006.

(2) Demir, S.; Jeon, I.-R.; Long, J. R.; Harris, T. D. Radical Ligand-Containing Single-Molecule Magnets. *Coord. Chem. Rev.* **2015**, *289–290*, 149–176.

(3) Kahn, O. *Molecular Magnetism*; Wiley-VCH, 1993.

(4) Venanzi, L. M. Transition Metal Complexes with Bridging Hydride Ligands. *Coord. Chem. Rev.* **1982**, *43*, 251–274.

(5) Selected reviews: (a) Cummins, C. C. Three-Coordinate Complexes of 'Hard' Ligands: Advances in Synthesis, Structure and Reactivity. *Prog. Inorg. Chem.* **2007**, *47*, 685–836. (b) Alvarez, S. Bonding and Stereochemistry in Three-Coordinated Transition Metal Compounds. *Coord. Chem. Rev.* **1999**, *193–195*, 13–41. (c) Power, P. P. Some Highlights from the Development and Use of Bulky Monodentate Ligands. *J. Organomet. Chem.* **2004**, *689*, 3904–3919. (d) Power, P. P. Stable Two-Coordinate, Open-Shell (d^1-d^9) Transition Metal Complexes. *Chem. Rev.* **2012**, *112*, 3482–3507. (e) Chen, C.; Bellows, S. M.; Holland, P. L. Tuning Steric and Electronic Effects in Transition Metal β-Diketiminate Complexes. *Dalton Trans.* **2015**, *44*, 16654–16670.

(6) (a) Klein, H.-F.; Mager, M.; Schmidt, A.; Hüber, M.; Haase, W.; Flörke, U.; Haupt, H.-J.; Boča, R. Synthesis, Structure, and Magnetic Properties of Low-Valent Triangulo Cobalt-Hydride Clusters $[XCo_3(\mu\text{-}CO)_3(PMe_3)_6]$. *Inorg. Chem.* **1997**, *36*, 4303–4306. (b) Kamiguchi, S.; Saito, T.; Mori, W. Magnetic Properties of the Octahedral Chromium Chalcogenide Cluster Complexes $[Cr_6Se_8(PEt_3)_6]$, $[Cr_6Se_8(H)(PEt_3)_2]$, and $[Cr_6S_8(H)(PEt_3)_2]$. *Bull. Chem. Soc. Jpn.* **2000**, *73*, 2487–2491. (c) Alzamly, A.; Gambarotta, S.; Korobkov, I.; Murugesu, M.; Le Roy, J. J. H.; Budzelaar, P. M. Isolation of a Hexanuclear Chromium Cluster with a Tetrahedral Hydridic Core and Its Catalytic Behavior for Ethylene Oligomerization. *Inorg. Chem.* **2014**, *53*, 6073–6081. (d) Anderton, K. J.; Ermert, D. M.; Quintero, P. A.; Turvey, M. W.; Fataftah, M. S.; Abboud, K. A.; Meisel, M. W.; Čižmár, E.; Murray, L. J. Correlating Bridging Ligand with Properties of Ligand-Templated $[Mn^{II}_3X_3]^{3+}$ Clusters (X = Br^-, Cl^-, H^-,MeO^-). *Inorg. Chem.* **2017**, *56*, 12012–12022.

(7) Fryzuk, M. D.; Leznoff, D. B.; Rettig, S. J.; Thompson, R. C. Magnetic Exchange in Dinuclear Chromium(II) Complexes: Effect of Bridging Chlorides and Bridging Hydrides in Antiferromagnetic Coupling. *Inorg. Chem.* **1994**, *33*, 5528–5534.

(8) Boča, R.; Klein, H.-F.; Schmidt, A.; Valko, M.; Linert, W. Magnetic Properties of Triangulo Cobalt–Hydride Cluster $[H_3Co(\mu_2\text{-}CO)_3(PMe_3)_6]$. *Chem. Phys. Lett.* **2000**, *323*, 243–248.

(9) Heintz, R. A.; Koetzle, T. F.; Ostrander, R. L.; Rheingold, A. L.; Theopold, K. H.; Wu, P. Unusually Strong Intramolecular Magnetic Coupling in a Chromium Hydride Cluster. *Nature* **1995**, *378*, 359–361.

(10) Yao, S. A.; Corcos, A. R.; Infante, I.; Hillard, E. A.; Clérac, R.; Berry, J. F. An "Intermediate Spin" Nickel Hydride Complex Stemming from Delocalized $Ni_2(\mu\text{-}H)_2$ Bonding. *J. Am. Chem. Soc.* **2014**, *136*, 13538–13541.

(11) Hayward, M. A.; Cussen, E. J.; Claridge, J. B.; Bieringer, M.; Rosseinsky, M. J.; Kiely, C. J.; Blundell, S. J.; Marshall, I. M.; Pratt, F. L. The Hydride Anion in an Extended Transition Metal Oxide Array: $LaSrCoO_3H_{0.7}$. *Science* **2002**, *295*, 1882–1884.

(12) Hickey, A. K.; Lee, W.-T.; Chen, C.-H.; Pink, M.; Smith, J. M. A Bidentate Carbene Ligand Stabilizes a Low-Coordinate Iron(0) Carbonyl Complex. *Organometallics* **2016**, *35*, 3069–3073.

(13) (a) Lee, W.-T.; Jeon, I.-R.; Xu, S.; Dickie, D. A.; Smith, J. M. Low-Coordinate Iron(II) Complexes of a Bulky Bis(carbene)borate Ligand. *Organometallics* **2014**, *33*, 5654–5659. (b) Hickey, A. K.; Lutz, S. A.; Chen, C.-H.; Smith, J. M. Two-State Reactivity in C-H Activation by a Four-Coordinate Iron(0) Complex. *Chem. Commun.* **2017**, *53*, 1245–1248. (c) Martinez, J. L.; Lee, W.-T.; Pink, M.; Chen, C.-H.; Smith, J. M. Heteroleptic Nickel Complexes of a Bulky Bis(carbene)borate Ligand. *Polyhedron* **2018**, *156*, 297–302.

(14) (a) Muller, G.; Sales, J.; Vinaixa, J.; Tejada, J. Mössbauer Spectra of Square-planar Organometallic Compounds of Iron(II). *Inorg. Chim. Acta* **1982**, *60*, 227–230. (b) Hawrelak, E. J.; Bernskoetter, W. H.; Lobkovsky, E.; Yee, G. T.; Bill, E.; Chirik, P. J. Square Planar vs Tetrahedral Geometry in Four Coordinate Iron(II) Complexes. *Inorg. Chem.* **2005**, *44*, 3103–3111. (c) Liu, Y.; Luo, L.; Xiao, J.; Wang, L.; Song, Y.; Qu, J.; Luo, Y.; Deng, L. Four-Coordinate Iron(II) Diaryl Compounds with Monodentate *N*-Heterocyclic Carbene Ligation: Synthesis, Characterization, and Their Tetrahedral-Square Planar Isomerization in Solution. *Inorg. Chem.* **2015**, *54*, 4752–4760. (d) Wang, L.; Cheng, J.; Deng, L. A Square Planar Iron(II) Biphenyl-2,20-diyl Complex with NHC Ligation: Synthesis, Characterization, and its Reactivity Toward Unsaturated Organic Substrates. *Inorg. Chim. Acta* **2017**, *460*, 49–54.

(15) (a) Smith, J. M.; Lachicotte, R. J.; Holland, P. L. N≡N Bond Cleavage by a Low-Coordinate Iron(II) Hydride Complex. *J. Am. Chem. Soc.* **2003**, *125*, 15752–15753. (b) Vela, J.; Smith, J. M.; Yu, Y.; Ketterer, N. A.; Flaschenriem, C. J.; Lachicotte, R. J.; Holland, P. L. Synthesis and Reactivity of Low-Coordinate Iron(II) Fluoride Complexes and Their Use in the Catalytic Hydrodefluorination of Fluorocarbons. *J. Am. Chem. Soc.* **2005**, *127*, 7857–7870. (c) Yu, Y.; Sadique, A. R.; Smith, J. M.; Dugan, T. R.; Cowley, R. E.; Brennessel, W. W.; Flaschenriem, C. J.; Bill, E.; Cundari, T. R.; Holland, P. L. The Reactivity Patterns of Low-Coordinate Iron-Hydride Complexes. *J. Am. Chem. Soc.* **2008**, *130*, 6624–6638. (d) Dugan, T. R.; Holland, P. L. New Routes to Low-Coordinate Iron Hydride Complexes: The Binuclear Oxidative Addition of H_2. *J. Organomet. Chem.* **2009**, *694*, 2825–2830. (e) Rodriguez, M. M.; Bill, E.; Brennessel, W. W.; Holland, P. L. N_2 Reduction and Hydrogenation to Ammonia by a Molecular Iron-Potassium Complex. *Science* **2011**, *334*, 780–783. (f) Dugan, T. R.; Bill, E.; MacLeod, K. C.; Brennessel, W. W.; Holland, P. L. Synthesis, Spectroscopy, and Hydrogen/Deuterium Exchange in High-Spin Iron(II) Hydride Complexes. *Inorg. Chem.* **2014**, *53*, 2370–2380. (g) Gehring, H.; Metzinger, R.; Braun, B.; Herwig, C.; Harder, S.; Ray, K.; Limberg, C. An Iron(II) Hydride

DOI: 10.1021/jacs.9b04389
J. Am. Chem. Soc. 2019, 141, 11970–11975

Complex of a Ligand with Two Adjacent β-Diketiminate Binding Sites and its Reactivity. *Dalton Trans.* **2016**, *45*, 2989−2996. (h) Bellows, S. M.; Arnet, N. A.; Gurubasavaraj, P. M.; Brennessel, W. W.; Bill, E.; Cundari, T. R.; Holland, P. L. The Mechanism of N−N Double Bond Cleavage by an Iron(II) Hydride Complex. *J. Am. Chem. Soc.* **2016**, *138*, 12112−12123. (i) Hein, N. M.; Pick, F. S.; Fryzuk, M. D. Synthesis and Reactivity of a Low-Coordinate Iron(II) Hydride Complex: Applications in Catalytic Hydrodefluorination. *Inorg. Chem.* **2017**, *56*, 14513−14523.

(16) $\tau_4 = (360 - \beta - \alpha)/141$. See: Yang, L.; Powell, D. R.; Houser, R. P. Structural Variation in Copper(I) Complexes with Pyridylmethylamide Ligands: Structural Analysis with a New Four-Coordinate Geometry Index, τ_4. *Dalton Trans.* **2007**, 955−964.

(17) Continuous shape measures also support these conclusions. For Fe(1) $S(D_{4h}) = 1.2$, $S(T_d) = 29.0$, while for Fe(2) $S(D_{4h}) = 20.3$, $S(T_d) = 6.3$, see Cirera, J.; Alemany, P.; Alvarez, S. Mapping the Stereochemistry and Symmetry of Tetracoordinate Transition-Metal Complexes. *Chem. Eur. J.* **2004**, *10*, 190−207.

(18) To the best of our knowledge, there are only two examples of hydride dimers created from square planar and tetrahedral monomers. The magnetic properties of these molecules have not been investigated in any detail: (a) Pfirrmann, S.; Limberg, C.; Ziemer, B. A Low-Coordinate Nickel(II) Hydride Complex and Its Reactivity. *Dalton Trans.* **2008**, 6689−6691. (b) Dugan, T. R.; Goldberg, J. M.; Brennessel, W. W.; Holland, P. L. Low-Coordinate Cobalt Fluoride Complexes: Synthesis, Reactions, and Production from C-F Activation Reactions. *Organometallics* **2012**, *31*, 1349−1360.

(19) Pelmenschikov, V.; Gee, L. B.; Wang, H.; MacLeod, K. C.; McWilliams, S. F.; Skubi, K.; Cramer, S. P.; Holland, P. L. **H**igh-Frequency Fe−H Vibrations in a Bridging Hydride Complex Characterized by NRVS and DFT. *Angew. Chem., Int. Ed.* **2018**, *57*, 9367−9371. To the best of our knowledge, Fe−H vibrations in related complexes have only been observed by nuclear resonance vibrational spectroscopy (NRVS).

(20) See Supporting Information for more details.

(21) Consistent with this formulation, the electronic absorption spectrum of the complex can be interpreted as comprising d-d transitions of both metal centers as well as CT bands (see SI).

(22) (a) Boča, R. Magnetic Parameters and Magnetic Functions in Mononuclear Complexes Beyond the Spin-Hamiltonian Formalism. *Struct. Bonding (Berlin)* **2006**, *117*, 1−264. (b) Boča, R. Zero-Field Splitting in Metal Complexes. *Coord. Chem. Rev.* **2004**, *248*, 757−815.

(23) Chilton, N. F.; Anderson, R. P.; Turner, L. D.; Soncini, A.; Murray, K. S. PHI: A Powerful New Program for the Analysis of Anisotropic Monomeric and Exchange-Coupled Polynuclear d- and f-Block Complexes. *J. Comput. Chem.* **2013**, *34*, 1164−1175.

(24) Magnetic susceptibility data were simulated with the following Hamiltonian: $\hat{H} = -2J[\hat{S}_{Fe1} \bullet \hat{S}_{Fe2})] + D_{Fe}(\hat{S}_{Fe1,z}{}^2 + \hat{S}_{Fe2,z}{}^2) + g\mu_B H(\hat{S}_{Fe1} + \hat{S}_{Fe2})$.

(25) The $S = 3$ ground state results from $S_1 + S_2 = 2 + 1 = 3$; there is also a lower energy excited state with $S = 2$ and the highest energy state with $S = 1$, from $|S_1 - S_2| = 2 - 1 = 1$.

(26) Low-temperature magnetization data were modeled according to the following Hamiltonian: $\hat{H} = D\hat{S}_z{}^2 + g_{iso}\mu_B \mathbf{S}\cdot\mathbf{B}$.

(27) (a) Telser, J.; Ozarowski, A.; Krzystek, J. High-Frequency and -Field Electron Paramagnetic Resonance of Transition Metal Ion (d block) Coordination Complexes. In *Electron Paramagnetic Resonance*; Gilbert, B. C.; Murphy, D. M.; Chechik, V., Eds.; RSC Publishing: Cambridge, 2013; Vol. 23, pp 209−263. (b) Krzystek, J.; Telser, J. Measuring Giant Anisotropy in Paramagnetic Transition Metal Complexes with Relevance to Single-Ion Magnetism. *Dalton Trans.* **2016**, *45*, 16751−16763.

(28) Heintz, R. A.; Neiss, T. G.; Theopold, K. H. Unusually Large Isotope Effects on NMR Chemical Shifts of Paramagnetic Organometallic Compounds. *Angew. Chem., Int. Ed. Engl.* **1994**, *33*, 2326−2328.

(29) Telser, J. EPR Interactions − Zero-Field Splittings. *eMagRes.* **2017**, *6*, 207−233.

(30) A more extensive analysis is provided in SI.

(31) It should be noted that this qualitative orbital diagram assumes that the two iron sites are isoenergetic, which is unlikely to be correct.

(32) Bencini, A.; Gatteschi, D. Xα-SW Calculations of the Electronic Structure and Magnetic Properties of Weakly Coupled Transition-Metal Clusters. The $[Cu_2Cl_6]^{2-}$ Dimers. *J. Am. Chem. Soc.* **1986**, *108*, 5763−5771.

DOI: 10.1021/jacs.9b04389
J. Am. Chem. Soc. 2019, 141, 11970−11975